Chulalongkorn University Dental Journal

Volume 27 | Issue 3 Article 1

2004-09-01

Comparison of ultimate tensile strength between torch soldering joints and laser welding joints in Au-Pd, Ni-Cr, and Co-Cr alloys

Pravej Serichetaphongse

Comparison of ultimate tensile strength between torch soldering joints and laser welding joints in Au-Pd, Ni-Cr, and Co-Cr alloys

Pravej Serichetaphongse D.D.S., M.S.

Department of Prosthodontics, Faculty of Dentistry, Chulalongkorn University

Abstract

Objective To compare the ultimate tensile strength of the soldering joint from conventional torch technique and the welding joint from laser technology in three types of alloy, gold-palladium (Au-Pd) alloy, nickle-chrome (Ni-Cr) alloy and cobalt-chrome (Co-Cr) alloy using the ISO standard model.

Materials and methods Fifty four specimens were prepared in accordance with ISO 6892 from three different alloys, Au-Pd alloy, Ni-Cr alloy and Co-Cr alloy. Six specimens of each alloy were cut and either soldered with gas propane-oxygen torch or welded with laser. The control group was six specimens without cutting (as cast specimens) of each alloy. All specimens were then undergone for thermocycling required for oxidation, opaque layer, dentine layer and glazing before testing. Specimens were tested for ultimate tensile strength (UTS) using universal testing machine. Scanning electron microscopy and energy dispersive x-ray microanalysis of the fractured surface were also obtained and evaluated.

Results The means ultimate tensile strength of laser welding specimens were higher than those of torch soldering specimens in all alloy groups (mean laser welding in Au-Pd group = 422.54 MPa, mean torch soldering in Au-Pd group = 279.33 MPa, mean control in Au-Pd group = 548.54 MPa, mean laser welding in Ni-Cr group = 600.99 MPa, mean torch soldering in Ni-Cr group = 395.06 MPa, mean control in Ni-Cr group = 549.42 MPa, mean laser welding in Co-Cr group = 646.67 MPa, mean torch soldering in Co-Cr group = 453.68 MPa and mean control in Co-Cr group = 672.13 MPa). Data analysis using one-way ANOVA and Bonferroni's test indicated that there were statistically significant differences ($p < .05$) of UTS between laser welding and solder specimens in all alloy groups while there was no statistically significant difference ($p < .05$) of ultimate tensile strength between welding joint and as cast in Ni-Cr alloy and Co-Cr alloy group.

Conclusion From this investigation, ultimate tensile strength of joint from laser welding technique was greater than that of a gas-propane oxygen torch soldering joint in Au-Pd, Ni-Cr and Co-Cr alloy. (CU Dent J 2004;27:171-81)

Key words: *alloy; laser welding; torch soldering; ultimate tensile strength; welding joint*

Poster presentation at 6th meeting of the International Congress on Maxillofacial Rehabilitation, 2004 Maastricht, Netherlands.

Introduction

Distortion of dental casting is usually occurred in prosthodontic dentistry such as in metal substructure of a long span bridge or in implant dentistry.[1-6] To solve this problem, the metal substructure needs to be cut and rejoined to get a passive fit. The common procedures to consolidate these metal components are either soldering or welding of metal or alloys.[7]

Soldering involves joining of filler alloy that has lower melting point 100°-150°C lower than the parent alloy to be joined by using either propane-oxygen torch called pre-soldering or oven heat called post-soldering technique. These techniques are time consuming and compromised precision.[8] The soldering joint showed inferior joint strength to one-piece casting due to air trap during melting alloy filler with torch and the impurity from flux material.[8] Since there is a composition difference between the solder and the parts, the joint is susceptible to galvanic corrosion leading to weakening joint in long term clinical use.[8]

Laser energy has been introduced and used in several areas of dentistry including joining of metal in dental laboratory work called laser welding technique.[9] Laser welding is a metallurgical joining process which relies on fusion of parent metals, with or without filler alloy.[9-11] The parental alloy can be used as filler material. The laser beam used in welding metal alloys produces by crystals of yttrium, aluminium, garnet (YAG) doped with neodymium (Nd). In dental laser welding machines (Nd:YAG laser), the output energy (voltage), pulse duration (millisecond) and spot diameter of the laser (millimeter) can be adjusted.[11] The combination of these three factors changes the penetration depth of the laser into the metal alloy and affects the mechanical joint strength. The success of laser welding procedure in dental alloys, however, depends on the control of these parameters.[11,12]

The thermal conductivity of the metal alloy is one of the factors that can affect the penetration depth of the welding metal alloy. The lower thermal conductivity of the alloy has a higher rate of laser beam absorption. Titanium has lower thermal conductivity (17 $Wm^{-1}C^{-1}$) and greater laser beam absorption (0.4%) compared to gold alloy which has higher thermal conductivity (297 $Wm^{-1}C^{-1}$) and lower laser beam absorption (0.03%).[12,13]

In addition to having stronger joint, laser welding joint is claimed to have advantages over conventional solder joint such as having higher corrosion resistance and obtaining precise welding. This technique can be used for any type of alloy and no requirement for neither solder flux material nor solder investment.[14,15]

None of previous studies has been investigated the strength of welding joint in three different metal alloys used for porcelain fusing using the casting model of ISO standard with simulated heat cycle of porcelain fabrication.

Objective

To compare the ultimate tensile strength of the joint formed by conventional torch soldering technique with those formed by laser technology in three types of alloy (Au-Pd , Ni-Cr and Co-Cr alloy) using the ISO standard model.

Materials and methods

A. Preparation of specimens

Eighteen test specimens in each of three different alloys; Au-Pd alloy (Bio Pontostar, batch no. 114070, Bego, Germany), Ni-Cr alloy (Bellabond, batch no. 205578, Bego, Germany), and Co-Cr alloy (Wirobond, batch no.1168, Bego, Germany) were cast in normal fashion to have a dimension according to ISO standard 6892 (Fig.1). The composition of each alloy was showed in Table 1. The ISO standard 6892 plastic patterns were sprued at both ends and invested with investment material (Bellavest, Bego, Germany) in the plastic ring. After 90 minutes, the investment was removed from the plastic ring and put in the burning oven at 300°C for 60 minutes to burn out the plastic pattern. Then the temperature was raised to 850°C for 60 minutes to be ready for Au-Pd alloy casting, 1,000°C for 60 minutes for Ni-Cr alloy casting and 1,000°C for 30 minutes for Co-Cr alloy casting respectively. All specimens were cast by casting machine (Nautilus, Bego, Germany). This particular casting machine operates on the principle of vacuum casting with an inductively heated melt. The temperature of melting metal was detected and measured by infrared radiation under a foaming gas (90% nitrogen and 10% hydrogen) to reduce oxide formation during melting metal and increase the accuracy of temperature measurement. The casting temperature was done under manufacturer instruction. The casting temperature was 1,030°C, 1,270°C and 1,470°C for Au-Pd, Ni-Cr and Co-Cr alloy group respectively. After casting, investment was removed and the

sprue was cut. The specimens were polished using rubber wheel and cleaned in the ultrasonic cleanser, then inspected under microscope at 20 X magnification. The poor castings were discarded.

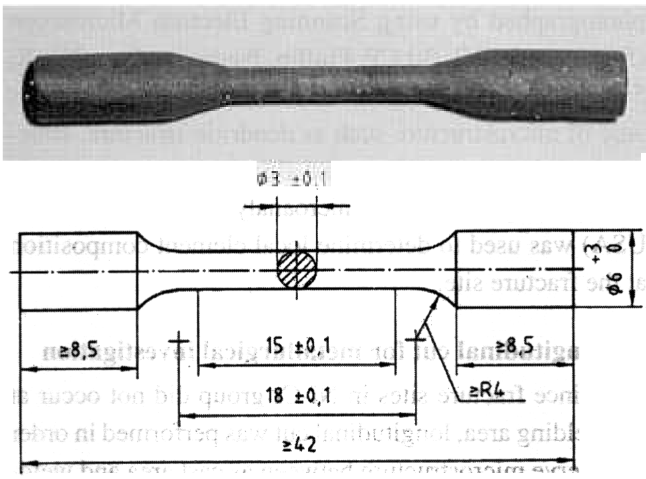

Figure 1 ISO standard dimension

Eighteen specimens in each alloy were randomly divided into three different groups as follows:

Group 1: The specimens without cutting was an as cast group. This group was used as a control group.

Group 2: Solder group. Each specimen was clamped by an aligning jig and cut to have a solder gap at 0.2 mm. The gap was filled with autopolymerizing resin (Duralay, Reliance Mfg., Worth) and allowed set at room temperature for 30 minutes. Then, specimen was boxed with wax and invested for soldering material (Bego soldering investment, Germany). After one hour, the wax was flushed with hot water and the resin was burned out at 500°C for 30 minutes. After cooling, the gap was cleaned and the investment was left to dry. The block was heated at 600°C for 40 minutes in the oven. Then, the propane oxygen soldering was performed in conventional manner with soldering material (Ponto Star® G-Solder, Bego, melting temperature at 1,030°C Germany for Au-Pd alloy, Wiron® solder, Bego, Germany for Ni-Cr alloy and Wirobond® solder, Bego, Germany for Co-Cr alloy respectively), (Fig. 2). Flux material was Minoxyd flux which contains potassium fluoride and sodium carbonate for Ni-Cr and Co-Cr group and Fluxsol flux which contains potassium fluoride, sodium carbonate and borax for Au-Pd group.

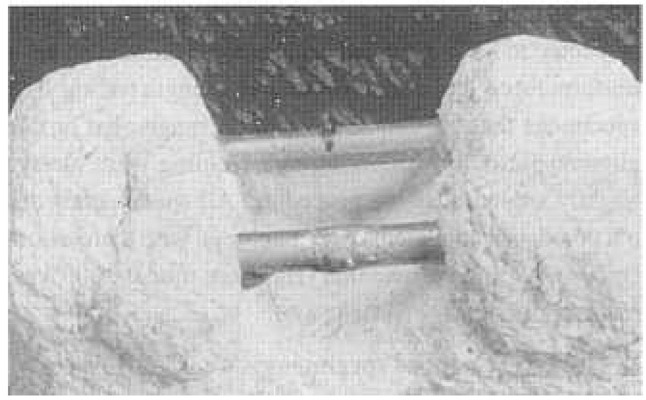

Figure 2 Torch soldering was performed under investment jig.

Group 3: Laser welding group: Each specimen was clamped into an aligning jig (Fig 3). It then was cut according to manufacturer's instruction and has a welding gap at 0.2 mm. Specimens were welded with laser welding machine, Nd:YAG laser, (Laser Star, BEGO, Germany; wavelength 1,064 nm.) with different parameters, according to type of alloy. For Au-Pd group, 0.5 - 0.8 mm diameter focal point, 270 - 290 volts and 8 - 12 milliseconds was used. For Ni-Cr group, 0.7 - 0.8 mm diameter focal point, 270 - 290 volts and 8 - 10 milliseconds was used. For Cr-Co group, 0.8 - 1 mm diameter focal point, 270 - 290 voltage and 7 milliseconds was used. The parent metal was used as a filler material in all alloy groups. Double sided laser welding technique was used to realign the specimen during laser welding procedure.[12]

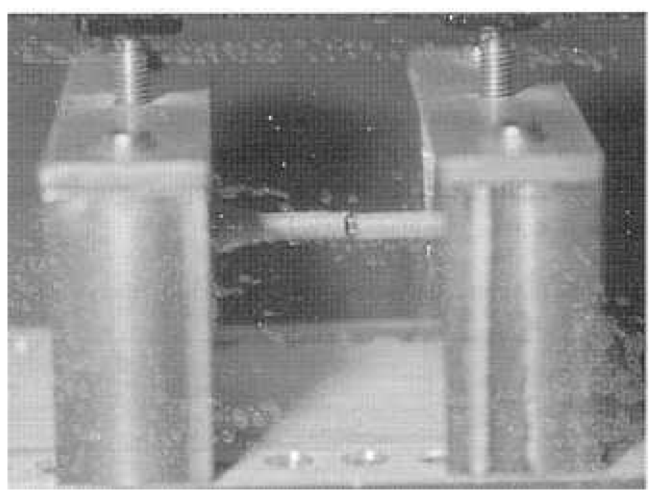

Figure 3 Laser welding was performed under an aligning jig.

Then all specimens in group 2 and 3 were cleaned in an ultrasonic cleanser and inspected under microscope at 20X magnification. All solder joints with surface defects were eliminated. All laser welding joint with surface voids were corrected by additional welding. After

soldering and welding procedure, all specimens were inspected to have a coaxial arrangement in order to get a uniform force application for tensile strength testing. The specimens that presented a coaxial arrangement on the aligning jig before soldering and welding were always slightly angled after the procedure. All specimens without coaxial arrangement were machined with a precision, centerless grinding machine (Hanison, model 300, West Yorkshire, UK).

B. Heat treatment of specimens

Heat treatment was performed using porcelain oven (Ivoclar Programat P100, Austria). All specimens were undergone thermal cycles required for oxidation (400°C - 980°C) for 5 minutes and vacuum for 3 minutes, opaque layer (400°C - 950°C) for 13 minutes and vacuum 6 minutes, dentine bake I (400 °C - 920°C) for 13 minutes and vacuum 6 minutes, dentine baked II (400°C - 910°C) for 13 minutes and vacuum 6 minutes, dentine baked III (400°C - 900°C) for 13 minutes and vacuum 6 minutes, glazing I (400°C - 895°C) for 7 minutes without vacuum, and glazing II (400°C - 895°C) for 7 minutes without vacuum.

C. Ultimate tensile strength testing

All specimens were conducted for ultimate tensile strength testing with universal testing machine (Instron, model 5583, Mainstreet Anytown, UK) with a crosshead speed of 3 mm per minute and a gauge length of 15 mm. The ultimate tensile strength (MPa) was recorded (Software Instron series 9 version 8.3) when specimen fractured, and the means and standard deviation were calculated (n = 6). The data were statistically analyzed using one way ANOVA and Bonferroni's Multiple Comparisons at the $p < .05$ significance level.

D. SEM and EDX observation

After tensile testing, two random specimens for each alloy group were taken (except a welding specimen of Ni-Cr group) and placed into the vacuum chamber of SEM-EDX system. Fractured surface was observed and photographed by using Scanning Electron Microscope (SEM, model XL 30 CP, Phillip, Netherland) at 250 X, 500 X and 1000 X magnifications to obtain the characteristic of microstructure such as dendritic structure, structural void, failure pattern and flux inclusion. The EDX (Energy Dispersive X-ray microanalysis machine; EDAX, USA) was used to determine local element composition at the fracture site.

E. Longitudinal cut for metallurgical investigation

Since fracture sites in Ni-Cr group did not occur at the welding area, longitudinal cut was performed in order to observe microstructure between as cast area and welding area. The similar procedure was performed in solder group in order to compare with welding group. Both soldering and welding specimens were then prepared for light metallography. Cut specimens were mounted in resin. The mounted specimens were then abraded by using silicon carbide papers from 220-1,200 grade and polished on cloth wheels using aluminium oxide particles mixing with water, then using 0.5 micron diamond spray and immersed in or swabbed with a mixed acid etch (Marble etchant: 10% CuSO4 in conc. 37% HCl and deionized water 50 ml) for 10 seconds. After etching, mounted specimens were rinsed with deionized water and dried. The surfaces from soldering and welding specimens were photographed with the scanning electron microscope (JSM-35 CF, Phillip, Holland) at 200-1,000 magnification and compared.

Table 1 Element compositions and thermal conductivity of tested alloy (Manufacturer's instruction)

	Compositions (%)							Thermal Conductivity ($Win^{-1}C^{-1}$)
Au-Pd	Au	Pt	Zu	In	Rh	Mn	Ta	270
(Bio PontoStar®)	87.0	10.6	.5	0.3	0.2	0.2	0.2	
NI-Cr	Ni	Cr	Mo	Nb	Fe	Al		90
(Bellabond®)	63.4	21.6	8.4	4.2	2.2	0.2		
	Co	Cr	Mo	W		Fe	Ce	
(Winbond®C)	61.0	26.0	6.0	5.0	1.0	0.5	0.5	90

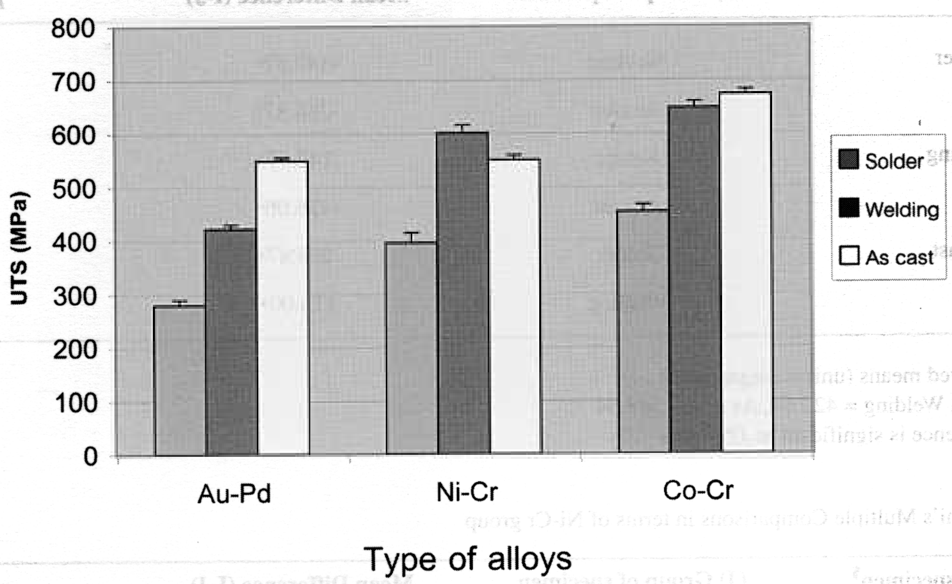

Figure 4 Ultimate tensile strenght; UTS (and standard deviation) between three alloys

Results

Ultimate tensile strength testing and determination

The means and standard deviations of the ultimate tensile strength (UTS) of three different alloy groups in as cast, laser welding and soldering specimens were shown in figure 4. The means UTS of laser welding specimens were higher than those of soldering specimens in all alloy groups. Using one-way ANOVA and Bonferroni's test, there were statistically significant differences ($p < .05$) of UTS between laser welding specimens and solder specimens in all alloy groups (Table 2 - 4). In Au-Pd alloy group, the mean UTS of as cast specimens (548.54 MPa) was the highest. The mean UTS of laser welding (422.54 MPa) was higher than that of soldering specimens (279.67 MPa). There was a statistically significant difference between as cast specimens and both welding and soldering specimens as well as between welding specimen and soldering specimens. In Co-Cr alloy group, the mean UTS of as cast specimens (672.13 MPa) was the highest. The UTS of welding specimens (mean = 646.67 MPa) was higher than that of soldering specimens (453.68 MPa). There was a statistically significant difference between soldering specimens and both welding and as cast specimens. However, there was no statistically significant difference between as cast specimens and welding specimens. In Ni-Cr alloy group, since the fracture site in welding specimens did not occur at the welding joint, the mean UTS of laser welding (600.99 MPa) was highest. The mean UTS of as cast specimens (549.4 MPa) was higher than that of soldering specimens (395.06 MPa). There was a statistically significant difference between as cast specimens and soldering specimens as well as between welding specimens and soldering specimens. There was no statistically significant difference between as cast and welding specimens.

Table 2 Bonferroni's Multiple Comparisons in terms of Au-Pd group

(I) Group of specimen$	(J) Group of specimen	Mean Difference (I-J)	*p*-value
	Welding	-142.87*	< .05
	As cast	-268.87*	< .05
Welding	Solder	142.87*	< .05
	As cast	-126.00*	< .05
	Solder	268.87*	< .05
	Welding	126.00*	< .05

$ Based on observed means (unit = megapascal)
Solder = 279.67, Welding = 422.54, As cast = 548.54
* The mean difference is significant at .05 levels

Table 3 Bonferroni's Multiple Comparisons in terms of Ni-Cr group

(I) Group of specimen$	(J) Group of specimen	Mean Difference (I-J)	*p*-value
	Welding	-205.93*	< .05
	As cast	154.36*	< .05
Welding	Solder	205.93*	< .05
	As cast	51.57*	NS#
As cast	Solder	154.36*	< .05
	Welding	-51.57*	NS#

$ Based on observed means (unit = megapascal)
Solder = 395.06, Welding = 609.99, As cast = 549.42
* The mean difference is significant at .05 levels
# NS = not significant

Table 4 Bonferroni's Multiple Comparisons in terms of Co-Cr group

(I) Group of specimen$	(J) Group of specimen	Mean Difference (I-J)	*p*-value
Solder	Welding	-192.99*	< .05
	As cast	-218.45*	< .05
Welding	Solder	192.99*	< .05
	As cast	-25.46	NS#
As cast	Solder	218.45*	< .05
	Welding	25.46	NS#

$ Based on observed means (unit = megapascal)
Solder = 453.68, Welding = 646.67, As cast = 672.13
* The mean difference is significant at 0.05 levels
# NS = not significant

SEM-EDX observation at fracture site

A. Au-Pd alloy group

As cast specimen, using SEM at 250 X magnification (Fig. 5a) showed dendritic microstructure. Solder specimen, at 500 X magnification showed of porosities and impurities (Fig. 5b). The porosities varied in size. The composition of impurities analyzed by EDX analysis showed calcium, sodium, chloride, and potassium elements which were composition of flux material (Fig. 5c). Welding specimen, at 1,000 X magnification showed no porosity or impurity (Fig. 5d). EDX analysis showed no contamination of other elements (Fig. 5e).

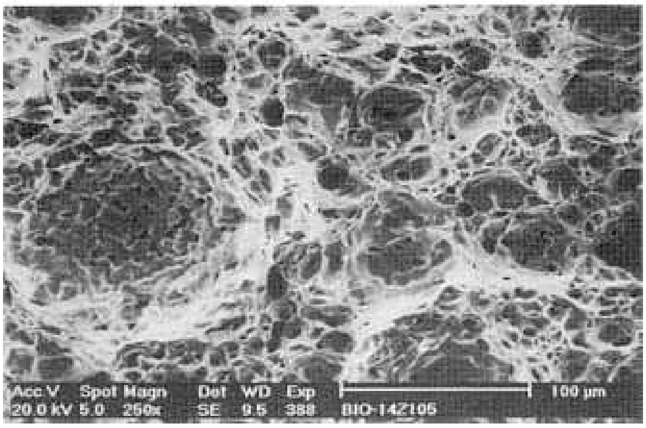

Figure 5a Au-Pd as cast specimen: SEM at 250 X showed dendritic microstructure.

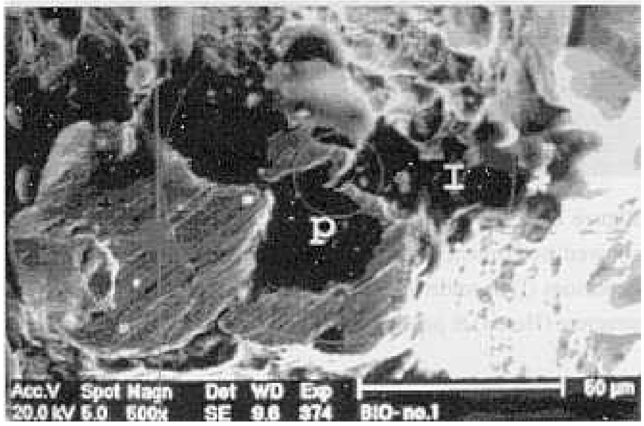

Figure 5b Au-Pd solder specimen: SEM at 500 X showed porostities (P = 28 miccrons) and impurities (I).

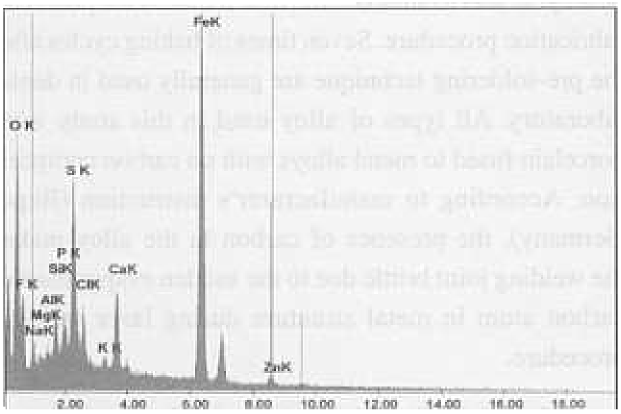

Figure 5c Au-Pd solder specimen: EDX showed contamination of flux materials (Ca, Cl, K and Na).

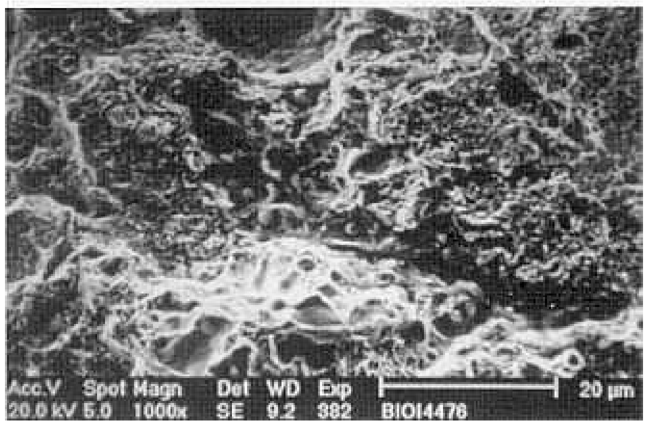

Figure 5d Au-Pd welding specimen: SEM at 1,000 X showed no porosity.

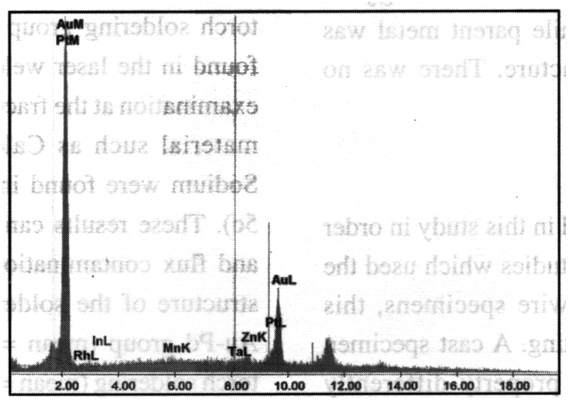

Figure 5e: Au-Pd welding specimen: EDX showed no contamination.

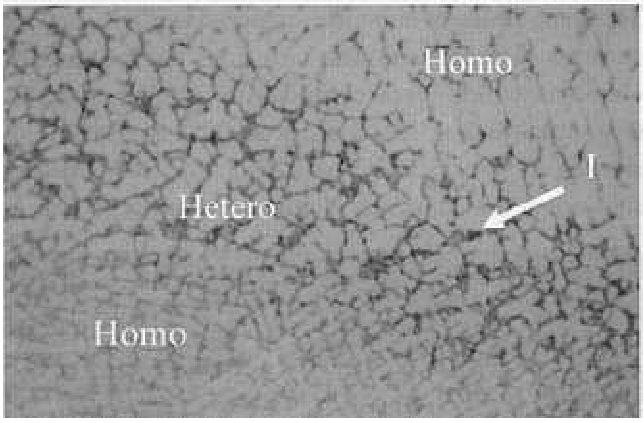

Figure 6a Ni-Cr longitudinal solder specimen: SEM at 200 X showed heterogeneous dendritic microstructure (Hetero) and impurities (I) at soldering area and homogenous dendritic microstructure (Homo) at parent metal area.

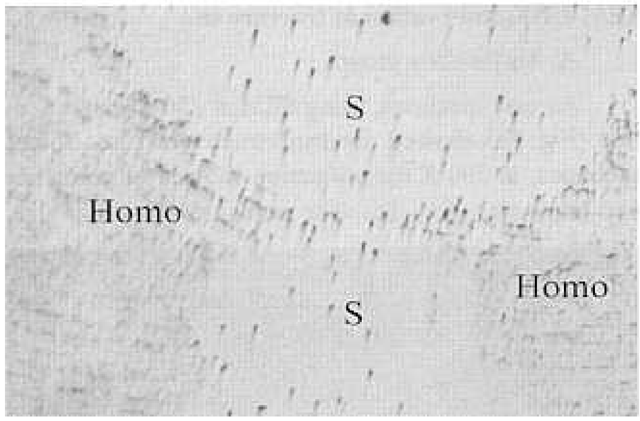

Figure 6b Ni-Cr longitudinal welding specimen: SEM at 50 X showed single crystal (S) in welding area and homogenous dendritic microstructure (Homo) at parent metal area.

B. Co-Cr alloy group

The findings in this group were similar to those in Au-Pd alloy group.

C. Ni-Cr alloy group

The findings in solder specimens were similar to those in Au-Pd alloy group in terms of porosities and impurities.

For welding specimen, which the fracture site did not occur at the welding area, a longitudinal cut specimen were performed as described before in both soldering and welding specimen. In a solder specimen, using SEM at 200 X magnification showed heterogeneous dendritic microstructure due to microshrinkage or microsegregation between dendrite structure and flux contamination compared to homogeneous dendritic microstructure in parent metal area (Fig. 6a). In welding specimen, using SEM at 50 X magnification, the microstructure of welding joint was more like a single crystal while parent metal was homogeneous dendritic microstructure. There was no impurity or porosity (Fig. 6b).

Discussion

ISO standard model was used in this study in order to compare the results with other studies which used the similar model. Instead of using wire specimens, this study used cast specimens for testing. A cast specimen has microstructure and ductility property differently from a wire specimen. Microstructure of a cast specimen is dendritic form while that of a wire specimen is a fine definite grain boundary. Therefore, the tensile and ductility of casting specimen were lower than those of wire specimens in previous studies.[14,15] The purpose of heat cycle was to simulate the heat required for porcelain fabrication procedure. Seven times of baking cycles after the pre-soldering technique are generally used in dental laboratory. All types of alloy used in this study were porcelain fused to metal alloys with no carbon composition. According to manufacturer's instruction (Bego, Germany), the presence of carbon in the alloy makes the welding joint brittle due to the sudden evaporation of carbon atom in metal structure during laser welding procedure.

In this study, the soldering joint showed lower strength than welding joint in all alloy groups. This result can be confirmed by SEM and EDX at the fracture site. From SEM of Au-Pd group, the porosity was found in the torch soldering group (Fig. 5b) while no porosity was found in the laser welding group (Fig. 5d). From EDX examination at the fracture site, the contamination of flux material such as Calcium, Potassium, Chloride and Sodium were found in torch soldering specimens (Fig. 5c). These results can be concluded that the porosities and flux contamination weakened the dendritic microstructure of the soldering area. The welding joint in Au-Pd group (mean = 422.54 MPa) was stronger than torch soldering (mean = 279.67 MPa) which corresponded to Watanabe's studies.[12,13] The similar finding in this study was also shown in both Ni-Cr and Co-Cr alloy

groups. However, in Ni-Cr group, the strength of the welding joint of Ni-Cr group (mean = 600.99 MPa) exceeded the strength of as cast group (mean = 549.42 MPa). The explanation from metallurgic observation of a welding specimen showed that the microstructure of welding joint was more like a single crystal while parent metal was homogeneous dendritic microstructure (Fig. 6b). It was thought that a rapid solidification of the melting alloy after the laser welding refined the grain, resulting in diminution of the grain size.[16] Soldering specimens (Ni-Cr alloy) showed heterogeneous dendritic microstructure due to microshrinkage or microsegregation between dendritic structure and flux contamination in solder area compared to homogeneous dendritic microstructure in parent metal area (Fig. 6a). That made the solder area less strength and brittle than parental area.[8,17,18]

The thermal conductivity affects the penetration depth of laser beam.[12, 13] The lower thermal conductivity of base metals (Co, Cr, Ni, Mo and Ti) has a greater rate of laser beam absorption than noble metals (Au, Ag, Pt and Pd). It was supported by data from this investigation. In Ni-Cr group, the joint strength of welding specimens showed higher strength than as cast specimens but had no statistically significant difference as well as in Co-Cr group, the joint strength of as cast specimens showed higher strength than welding specimens but there was no statistically significant difference. While as cast specimens showed significantly higher strength than welding specimens in Au-Pd group. This suggested that base metal alloy should be better candidates for laser welding compare to noble metal alloy.

According to the laser welding technique, author found that interaction between lasers and materials were very complex phenomena. The technician's dexterity and the choice of the welding parameter are recognized determinant of weld quality.[9,11] The welding parameter such as energy (voltage), time (millisecond) and focal point (diameter of welding point) need to be set up according to both type of work and alloy to get the best penetration of laser beam. These parameters must be set up according to manufacturer's recommendation. The laser technique requires a direct beam access to the joint. The pre-soldering is recommended for laser welding while post-soldering is not because of lack of direct access to the joint. The initial welding impact always distorts the coaxial arrangement, which can be reestablished by a second weld on the opposite site. Therefore, using laser welding technique, the precision of framework is compromised. Laser welding technique still needs a skillful technician to achieve the best result.

Conclusion

From this investigation, ultimate tensile strength of joint from laser welding technique was greater than that of a gas-propane oxygen torch soldering joint in Au-Pd, Ni-Cr and Co-Cr alloy.

Acknowledgements

Research grant was supported by Ministry of University Affairs.

Poster presentation was supported by Faculty of Dentistry, Chulalongkorn University

Technical support was kindly suggested by Dr. Roland Strietzel, Head of R&D Department and Mr. Jurgen Schultze, Technician in Bego Training Center (Bego Company, Germany) Dental Asia Company, Bangkok, Thailand

References

1. Jemt T. Three-dimensional distortion of gold alloy castings and welded titanium frameworks. Measurements of the precision of fit between completed implant prostheses and the master casts in routine edentulous situations. J Oral Rehabil 1995;22(8):557-64.
2. Tan KB, Rubenstein JE, Nicholis JI, Yuodelis RA. Three dimensional analysis of the casting accuracy of one-piece, osseointegrated implant-retained prostheses. Int J Prosthodont 1993;6(4):346-63.
3. Schiffleder BE, Ziebert GJ, DhuruVB, Brantley WA, Sigaroudi K. Comparison of accuracy of multi one-piece castings. J Prosthet Dent 1985;54(6):770-6.
4. Knabe C, Hoffmeister B. Implant-supported titanium prostheses following augmentation procedures: a clinical report. Aust Dent J 2003;48(1):55-60.
5. Tomotake Y, Ishida O, Kanitani H, Ichikawa T. Immediate implant-supported oral rehabilitation using a photocurable plastic skull model and laser welding. A technical note on the screw retained type: Part 1. Int J Prosthodont 2002;15(3):303-6.

6. Ishikawa M, Kashiwabara T, Ishida O, Ichikawa T. Installing magnetic keepers using laser welding. J Prosthodont 2002;11(1):49-52.
7. Huling JS, Clark RE. Comparative distortion in three-unit fixed prostheses joined by laser welding, conventional soldering, or casting in one piece. J Dent Res 1977;56920:128-34.
8. William J. O'Brien. Dental Materials and Their Selection. Illenoids: Quintessence Publishing Co, Inc., 1997:303-14.
9. Frentzen M, Koort HJ. Lasers in dentistry: new possibilities with advancing laser technology? Int Dent J 1990;40(6):323-32.
10. Wiskott HW, Macheret F, Bussy F, Belser UC. Mechanical and element characterization of solder joints and welds using a gold-palladium alloy. J Prosthet Dent 1997;77(6):607-16.
11. Bertrand C, Le Petitcorps Y, Albingre L, Dupuis V. Optimization of operator and physical parameters for laser welding of dental materials. Br Dent J 2004; 196(7):413-8.
12. Watanabe I, Liu J, Atsuta M, Okabe T. Effect of welding method on joint strength of laser-welded gold alloy. Am J Dent 2003;16(4):231-4.
13. Watanabe I, Liu J, Atsuta M. Effect of heat treatments on mechanical strength of laser-welded equi-atomic AuCu-6at%Ga alloy. J Dent Res 2001;80(9):1813-7.
14. Bertrand C, Le Petitcorps Y, Albingre L, Dupuis V. The laser welding technique applied to the non precious dental alloys. Br Dent J 2001;190(5):225-7.
15. Heidemann J, Witt E, Feeg M, Werz R, Pieger K. Orthodontic soldering techniques: aspects of quality assurance in the dental laboratory. J Orofac Orthop 2002; 63(4):325-38.
16. Phillips RW. Gold alloy solders. Soldering procedures. Science of dental materials. 8th ed. St. Louis, Missouri: W.B. Saunders Company, 1982:534-46.
17. Winkler S, Morris HFMonterio JM. Changes in mechanical properties and microstructure following heat treatment of a nickel-chromium base alloy. J Prosthet Dent 1984;52:821.
18. Civjan S, Huget EF, Godfrey GD, Lichtenberger H, Frank WA. Effects of heat treatment on mechanical properties of two nickel-chromium base casting alloys. J Dent Res 1972;51:1537.

การเปรียบเทียบกำลังดึงประลัยของจุดบัดกรีระหว่างวิธีบัดกรีด้วยไฟและเชื่อมด้วยเลเซอร์ในโลหะผสมทองพาเลเดียม นิเกิลโครม และโคบอลท์โครม

ประเวศ เสรีเชษฐพงษ์ ท.บ., M.S.

ภาควิชาทันตกรรมประดิษฐ์ คณะทันตแพทยศาสตร์ จุฬาลงกรณ์มหาวิทยาลัย

บทคัดย่อ

วัตถุประสงค์ ต้องการเปรียบเทียบค่ากำลังดึงประลัยระหว่างจุดบัดกรีด้วยเลเซอร์และจุดบัดกรีด้วยไฟของโลหะผสม 3 ชนิด (ทองพาเลเดียม, นิเกิลโครม และโคบอลท์โครม) โดยใช้ชิ้นงานตามมาตรฐานของ ISO

วัสดุและวิธีการ ชิ้นโลหะตัวอย่าง 54 ชิ้น ที่ผลิตจากโลหะผสม 3 ชนิด คือ ทองพาเลเดียม, นิเกิลโครม และโคบอลท์โครม ถูกเตรียมตามข้อกำหนดของ ISO 6892 ชิ้นงาน 6 ชิ้นจากโลหะผสมแต่ละชนิด ถูกนำไปตัดแล้วบัดกรีด้วยไฟจากแก๊สโพรเพนออกซิเจนและเชื่อมด้วยเลเซอร์ ชิ้นงานอีก 6 ชิ้นงานที่ไม่มีจุดบัดกรีของโลหะผสมแต่ละชนิดถือเป็นกลุ่มควบคุม จากนั้นนำชิ้นตัวอย่างทั้งหมดผ่านขบวนการทางความร้อนเลียนแบบการทำโอเปค ขั้นเดนทีน และเคลือบผิวก่อนทำการทดสอบ และนำชิ้นงานทั้งหมดมาทดสอบโดยการดึงด้วยเครื่องอินสตรอน เพื่อหาค่ากำลังดึงประลัย และใช้กล้องจุลทรรศน์อิเลคตรอนรวมทั้งใช้เครื่องตรวจวิเคราะห์ธาตุตรวจดูและวิเคราะห์บริเวณรอยหัก

ผลการศึกษา ค่าเฉลี่ยของกำลังดึงประลัยจากการเชื่อมด้วยเลเซอร์สูงกว่าค่าเฉลี่ยกำลังดึงประลัยของการบัดกรีด้วยไฟในโลหะผสมทั้ง 3 ชนิด (ค่าเฉลี่ยของการเชื่อมด้วยเลเซอร์เป็น 422.54 เมกกะปาสคาล ค่าเฉลี่ยของการบัดกรีด้วยไฟเป็น 279.33 เมกกะปาสคาล และค่าเฉลี่ยของกลุ่มควบคุมเป็น 548.54 เมกกะปาสคาล ในกลุ่มของโลหะผสมทองพาเลเดียม ค่าเฉลี่ยของการเชื่อมด้วยเลเซอร์เป็น 600.99 เมกกะปาสคาล ค่าเฉลี่ยของการบัดกรีด้วยไฟเป็น 395.06 เมกกะปาสคาล และค่าเฉลี่ยของกลุ่มควบคุมเป็น 549.42 เมกกะปาสคาล ในกลุ่มโลหะผสมนิเกิลโครม และค่าเฉลี่ยของการเชื่อมด้วยเลเซอร์เป็น 646.67 เมกกะปาสคาล ค่าเฉลี่ยของการบัดกรีด้วยไฟเป็น 453.68 เมกกะปาสคาลและค่าเฉลี่ยของกลุ่มควบคุมเป็น 672.13 เมกกะปาสคาล ในกลุ่มโลหะผสมโคบอลท์โครม) จากการวิเคราะห์ผลโดยใช้สถิติการวิเคราะห์ความแปรปรวนแบบทางเดียว และแบบบอนเฟอร์โรไน พบว่า มีความแตกต่างอย่างมีนัยสำคัญ ($p < .05$) ระหว่างการเชื่อมด้วยเลเซอร์ และการบัดกรีด้วยไฟในกลุ่มโลหะผสมทั้งสามชนิด และไม่มีความแตกต่างอย่างมีนัยสำคัญ ($p < .05$) ระหว่างกลุ่มควบคุมและกลุ่มที่เชื่อมด้วยเลเซอร์ของโลหะผสมนิเกิลโครมและโคบอลท์โครม

สรุป จากการทดลองพบว่าจุดเชื่อมด้วยเลเซอร์มีความแข็งแรงต่อการดึงมากกว่าจุดบัดกรีด้วยไฟในโลหะผสมทั้งสามชนิด

(ว ทันต จุฬาฯ 2547;27:171-81)

คำสำคัญ: *การเชื่อมด้วยเลเซอร์ การบัดกรีด้วยไฟ กำลังดึงประลัย จุดเชื่อมด้วยเลเซอร์ โลหะผสม*